

# Multimatrix Variation Matrix-Assisted Laser Desorption/Ionization Mass Spectrometry as a Tool for Determining the Bonding of Nitrogen Atoms in Alkaloids

Tohru Yamagaki,\* Tsukiho Osawa, Kohki Fujikawa, Takehiro Watanabe, and Kohtaro Sugahara

Cite This: *J. Am. Soc. Mass Spectrom.* 2022, 33, 2243–2249

Read Online

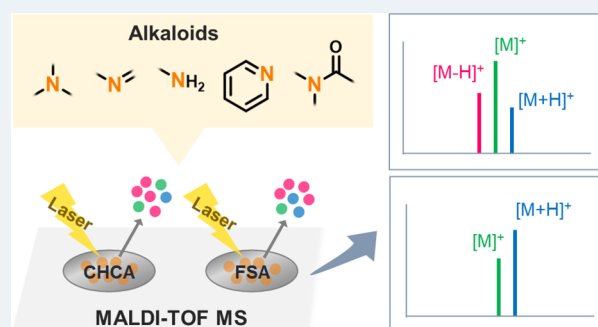
ACCESS |

 Metrics & More

 Article Recommendations

 Supporting Information

**ABSTRACT:** The reactivity of alkaloids in dehydrogenation was investigated using multimatrix variation matrix-assisted laser desorption/ionization mass spectrometry (MALDI-MS) of over 20 different alkaloids with six matrices. The dehydrogenated molecular ions  $[M - H]^+$  generated by in-source decay were detected in the MALDI mass spectra of some types of alkaloids such as reserpine. The dehydrogenation proceeded at the cyclic tertiary amine rather than double-bonded nitrogen atoms and indole rings involved in the electron-delocalized systems. The stable protonated primary amines hindered dehydrogenation. The laser-induced dehydrogenation correlated with the chemical properties and structures of alkaloids. Alkaloids were classified into three types by the ratio of dehydrogenation by comparing the relative abundances of  $[M - H]^+$ ,  $[M]^{*+}$ , and  $[M + H]^+$  ions in  $\alpha$ -cyano-4-hydroxycinnamic acid and 5-formylsalicylic acid matrices. Structural isomers were also discriminated by this method of analyzing the three molecular ions' ratio using multimatrix variation MALDI-MS.



Matrix-assisted laser desorption/ionization mass spectrometry (MALDI-MS) is one of the most useful tools for the identification of biomolecules such as metabolites. MALDI-MS is also applied for imaging mass spectra of the metabolites on a biological tissue section.<sup>1–3</sup> Nowadays, MALDI-MS is an essential technique for imaging small molecules.<sup>3–7</sup> When small molecules are ionized by MALDI, a few molecular ions and/or in-source decay ions may be generated, such as  $[M - H]^+$ ,  $[M]^{*+}$ , and  $[M + H]^+$ , in the positive mode. Compounds with aromatic rings were easily ionized as the molecular ion  $[M]^{*+}$ , and the base or acid compounds were easily ionized to the protonated/deprotonated molecules  $[M + H]^+/[M - H]^-$ .<sup>8</sup> Previously, it was reported that  $[M - H]^+$  ions generated by fast bombardment (FAB) were identified in mass spectra of cholesterol,<sup>9,10</sup>  $\alpha$ -tocopherol, and trolox.<sup>11</sup> The complex  $[M - H]^+$ ,  $[M]^{*+}$ , and  $[M + H]^+$  molecular related ions of alkaloids were generated by fast bombardment of the nitrogen-containing compounds in fossil fuel.<sup>12</sup> The hydrogen radical removal in the negative-ion polyphenols such as  $[M - H - H]^{*-}$  ion species was observed by MALDI-MS,<sup>8,13,14</sup> while the hydrogen radical removal from the phenolic hydroxy groups was registered by in-source decay MALDI-MS. The H removal correlated with the structure, and different isomers of flavonoid-glycosides and dihydroxybenzoic acids were identified from MALDI mass spectra by laser-induced hydrogen radical removal.<sup>14</sup>

Reserpine is an indole alkaloid (Figure 1) extracted from the Indian plant *Rauwolfia serpentina* used as a tranquilizer and antihypertensive drug. Interestingly, the  $[M - H]^+$  ion was abundant from in-source decay and the molecular related ions  $[M]^{*+}$  and  $[M + H]^+$  in the present work in positive-ion MALDI-MS without matrix. Alternatively, the  $[M + H + 2]^+$  ions were detected in the MALDI mass spectra of pyridyl-aminated oligosaccharides.<sup>15</sup> Previously, Nonami et al. investigated  $\beta$ -carboline alkaloids and pyrido-, pyridyl-, and pyridylpyridoindoles as new effective matrices in MALDI-MS; however, the  $[M - H]^+$  ions of these alkaloids were not reported in their MALDI-MS.<sup>16,17</sup> The question was whether the  $[M - H]^+$  ion was generally generated in all alkaloids or in only a specific structure of alkaloids. It was important for the structure identification or annotations of unknown compounds. The unexpected  $[M - H]^+$  ion would hinder the identification of the alkaloid analytes. The aim was to determine the required structure of alkaloids to produce the  $[M - H]^+$  ion by MALDI-MS. The abundance ratio of the three molecular ions  $[M - H]^+$ ,  $[M]^{*+}$ , and  $[M + H]^+$  was an

**Received:** August 6, 2022  
**Revised:** October 18, 2022  
**Accepted:** November 2, 2022  
**Published:** November 15, 2022



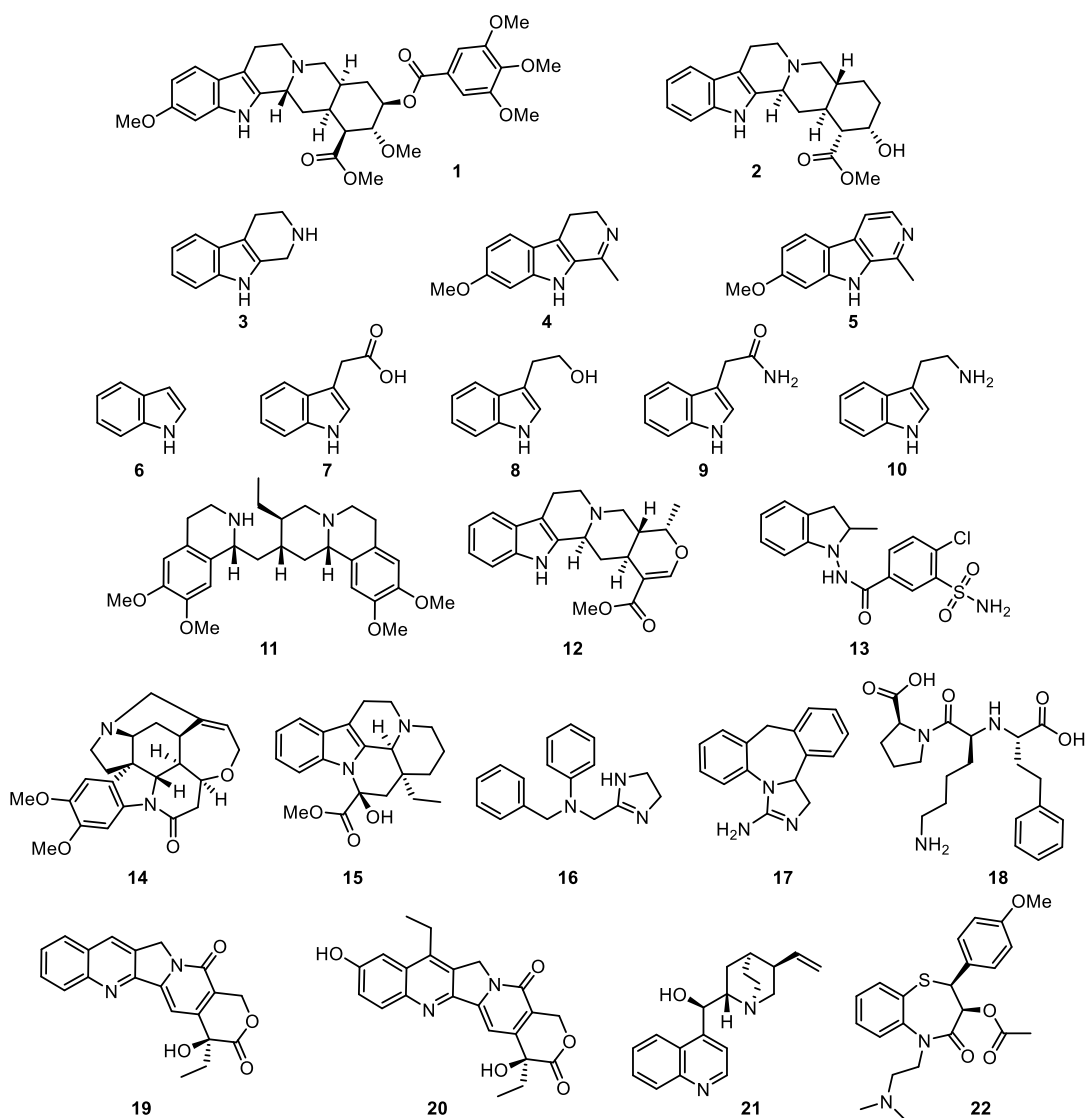


**Figure 1.** Structure of alkaloids: reserpine (1), yohimbine (2), tryptoline (3), harmaline (4), harmine (5), indole (6), indole-3-acetic acid (7), indole-3-ethanol (8), indole-3-acetamide (9), tryptamine (10), emetine (11), ajmalicine (12), indapamide (13), brucine (14), vincamine (15), antazoline (16), epinastine (17), lisinopril (18), camptothecin (19), 7-ethyl 10-hydroxycamptothecin (20), cinchonidine (21), and diltiazem (22).

indicator of the reactivity of alkaloids in the multimatrix variation MALDI-MS. This reactivity indicated the bonding types of the nitrogen atom, which were used in the structural analysis and isomer discrimination of alkaloids.

## EXPERIMENTAL SECTION

**Materials.** Methanol of HPLC grade, indole-3-acetic acid, yohimbine, and reserpine were purchased from Nacalai Tesque, Inc., Kyoto, Japan. Harmine hydrochloride, harmaline, indole-3-ethanol, indole-3-acetamide, 5-nitrosalicylic acid (NSA), 1,5-diaminonaphthalene (DAN), 5-aminosalicylic acid (ASA), and 5-formylsalicylic acid (FSA) were purchased from Tokyo Chemical Industry Co. Ltd., Tokyo, Japan. Tryptamine was purchased from Cayman Chemical Company, Ann Arbor, MI, USA. 2,5-Dihydroxybenzoic acid (DHB) for MALDI-MS and  $\alpha$ -cyano-4-hydroxycinnamic acid (CHCA) were purchased from Sigma-Aldrich Co., LLC, St. Louis, MO, USA. 1,2,3,4-Tetrahydro-9H-pyrido[3,4-*b*]indole (tryptoline) and brucine were purchased from Chem-Impex Intl, Inc., Wood Dale, IL, USA. Indapamide, vincamine, *cis*-diltiazem, antazoline-HCl,

cinchonidine, lisinopril dihydrate, and 7-ethyl-10-hydroxycamptothecin were purchased from Tokyo Chemical Industry Co. Ltd., Tokyo, Japan. Epinastine was purchased from BLD Pharmatech Ltd., Shanghai, P.R. China. Ajmalicine was purchased from Extrasynthese S.A., Lyon, France. Camptothecin was purchased from Alomone Laboratories, Israel. The molecular formula and mono isotopic molecular mass of all analytes are summarized in the [Supporting Information Table SI-1](#). Water was produced by an ultrapure water production system of Milli-Q IQ 7003 (Merck KGaA, Darmstadt, Germany) with ion-exchange filtration by activated carbon.

**Mass Spectrometry.** All MS spectra were acquired from a RapifleX MALDI-TOF/TOF tandem MS/MS instrument (Bruker Corp., Billerica, MA, USA) in the reflectron and positive-ion mode in the 0–2 kDa range. The laser was a Smartbeam 3D laser with a wavelength of 355 nm and laser energy of  $>100 \mu\text{J}/\text{pulse}$ . The ion acceleration was 20 kV as the ion source 1, the lens was 11.5 kV, and the reflectron 1 was 20.83 kV. The mass spectra of 10000 laser shots were accumulated at the different area each 2000 laser shots as one

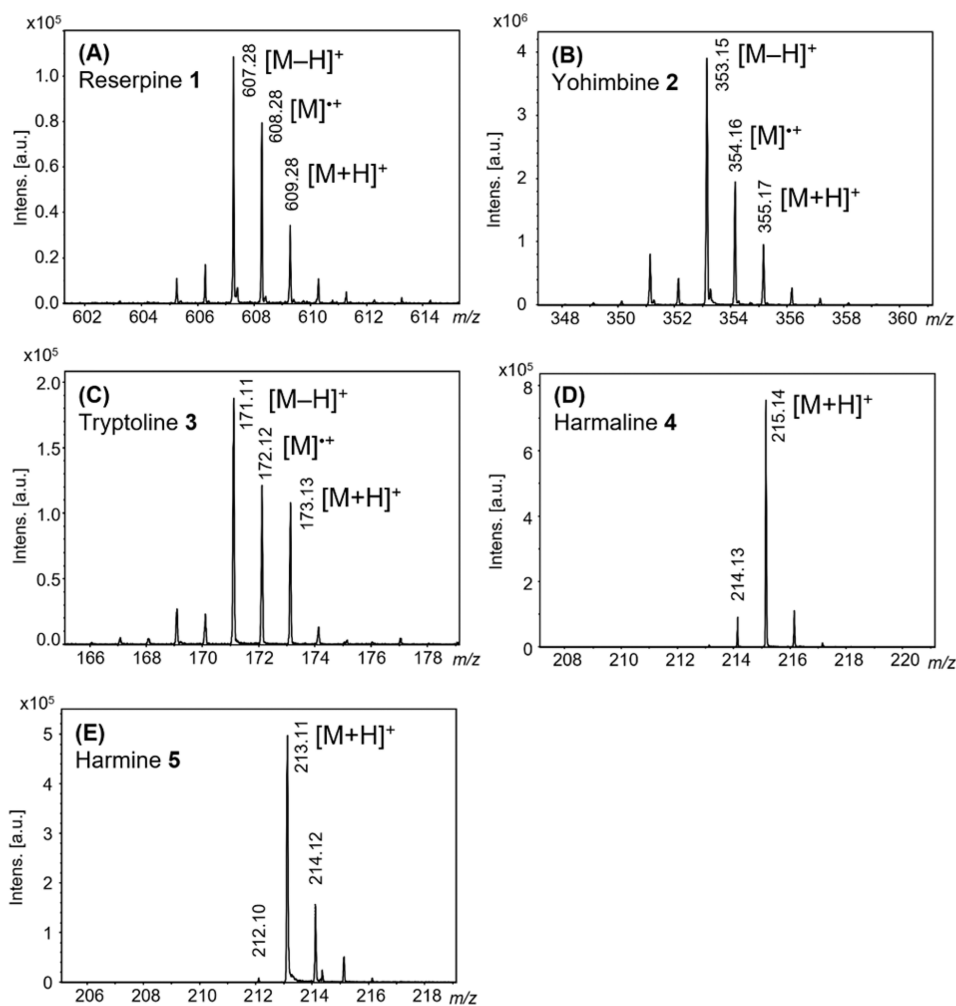


**Figure 2.** MALDI-MS spectra of alkaloids **1** (A), **2** (B), **3** (C), **4** (D), and **5** (E). Relative intensities of the  $[M - H]^+$ ,  $[M]^{++}$ , and  $[M + H]^+$  ions were compared between alkaloids **1**–**5**.

mass spectrum. The laser irradiation power was controlled with an attenuation filter of the instrument, and the power values were shown as percentage (%) of the laser output (100%). The experimental laser powers were optimized without signal broadening and overirradiation in each analyte, and each matrix is summarized in [Supporting Information Table SI-2](#). The optimized laser powers tended to be dependent on the matrices mainly.

**Sample Preparation.** All six matrices (DHB,<sup>18</sup> CHCA,<sup>19</sup> DAN,<sup>20</sup> ASA,<sup>21</sup> FSA,<sup>22</sup> and NSA,<sup>22</sup> their structures are presented in [Supporting Information SI-3](#)), each 50 mM, were dissolved in 60% methanol solution by sonication in hot water. All analytes with 5 mM concentrations were dissolved and/or suspended in 60% methanol solution by the same procedure. Five microliter aliquots of the analytes were premixed with 50  $\mu$ L of the matrix and 45  $\mu$ L of 60% methanol (total volume of each solution was 100  $\mu$ L) where the analyte and matrix concentrations were 0.25 mM. One microliter aliquots of the premixed solutions were deposited on the target plate. The analytes of auxin metabolites, indole, indole-3-ethanol, indole-3-acetic acid, indole-3-acetamide, and tryptamine were measured in the higher concentration of the premixed solution because they were small molecules close to the matrix. A total of 20  $\mu$ L aliquots of each analyte were premixed with the same aliquots of 50 mM CHCA, and 1  $\mu$ L

aliquots of the premixed solutions were deposited on the target plate.

## RESULTS AND DISCUSSION

The theoretical position of the peak of  $[M + H]^+$  monoisotopic ion in the protonated molecule of Reserpine **1** ( $C_{33}H_{40}N_2O_9$ ) is at  $m/z$  609.28; however, the peak is shifted to  $m/z$  607.28 on the MALDI-MS spectra ([Figure 2](#)). The dominant peak of  $[M - H]^+$  in-source decay ion at  $m/z$  607.28 is accompanied by the peaks of the molecular ion  $[M]^{++}$  at  $m/z$  608.28 and protonated molecule  $[M + H]^+$  at  $m/z$  609.28 in the spectrum of **1** without matrix as shown in [Figure 2A](#) and [SI-4](#). The  $[M - H]^+$  ion was unexpectedly formed by dehydrogenation of the protonated molecule  $[M + H]^+$  and/or the molecular ion  $[M]^{++}$ . At first, we tried to reveal where the dehydrogenation occurred in the structure of **1**.

**Effects of the Galloyl Group: Yohimbine.** In yohimbine **2** ( $C_{21}H_{26}N_2O_3$ ), an indole alkaloid extracted from a middle African plant *Rubiaceae* of *Pausinystalia yohimbe*, the galloyl group is missing as compared to the structure of **1**. By analogy to **1**, the spectrum of **2** is dominated by the peak of dehydrogenated ion  $[M - H]^+$  at  $m/z$  353.15 ([Figure 2B](#)). Therefore, the dehydrogenation did not proceed in the galloyl group.

**Tryptoline, Harmaline, and Harmine.** Tryptoline **3**, harmaline **4**, and harmine **5** are the parts of the **1** and **2** structures containing an indole ring with different cyclic amino groups. Interestingly, only the protonated molecules  $[M + H]^+$  were registered by MALDI-MS of **4** and **5** without matrix (Figure 2) in sharp contrast with the spectra of **1** and **2**. On the other hand, the dehydrogenated ion  $[M - H]^+$  was generated from **3**, and its spectrum was similar to those of **1** and **2**. Therefore, the indole ring was not involved in the dehydrogenation because **1**–**5** compounds have the same indole ring (Figure 1). At the same time, the double bond near the nitrogen in **4** and **5** inhibited their dehydrogenation, certifying that the C–N–C single bond in the ring is needed for the alkaloid dehydrogenation in in-source decay MALDI. The single-bonded nitrogen atom was protonated followed by the removal of the hydrogen atoms bonded to the  $\alpha$ -carbon and nitrogen atoms.

Therefore, the dehydrogenation of alkaloids was dependent on their structure, namely the type of nitrogen atom bonds (single or double). Therefore, the laser-induced dehydrogenation of alkaloids provided useful information to predict the structure of alkaloids.

#### Matrix Effects on Dehydrogenation of Alkaloids.

Figure 3 shows the MALDI-MS spectra of **1** with various matrices. The entire mass spectrum from  $m/z$  100 to 800 is shown in SI-4. The abundance of molecular related ions shifted from  $[M + H]^+$  to  $[M - H]^+$  ions when the matrices were

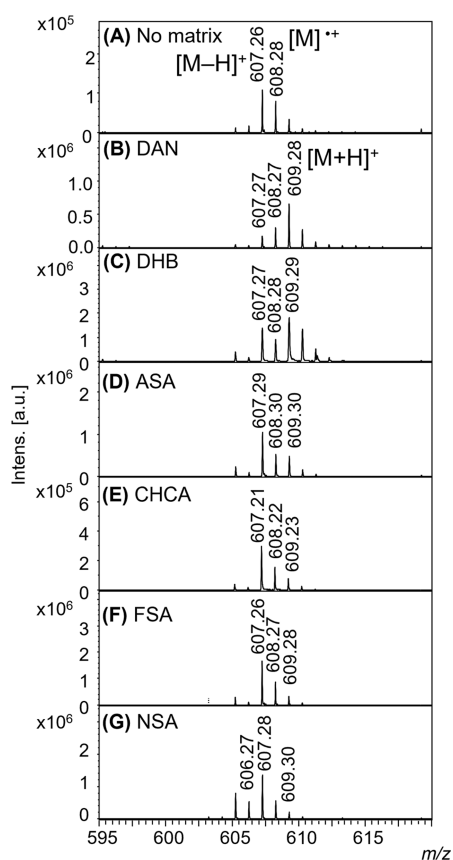


**Figure 3.** MALDI-MS spectra of reserpine **1** without matrix (A) and with DAN (B), DHB (C), ASA (D), CHCA (E), FSA (F), and NSA (G) matrices. Relative intensities of the  $[M - H]^+$  at  $m/z$  606.2,  $[M]^+$  at  $m/z$  607.2, and  $[M + H]^+$  ion at  $m/z$  609.3 were compared between the six spectra with the different six matrices.

switched in the sequence of DAN, DHB, ASA, CHCA, FSA, and NSA (their structures are summarized in SI-3). The matrices directly influenced the dehydrogenation of **1** in MALDI-MS, and the extent of the dehydrogenation correlated with their chemical properties. DAN was a reductive matrix.<sup>23</sup> The peptides with disulfide bonds were reduced by DAN, and the  $[M + H + 2H]^+$  ions were detected in the DAN-MALDI mass spectra previously.<sup>23</sup>

The dehydrogenation of **1** was mostly suppressed in the DAN-MALDI mass spectrum, and the  $[M + H]^+$  ion was the most abundant as shown in Figure 3(B) due to the DAN reducing property.<sup>23</sup> The  $[M - H]^+$  and  $[M + H]^+$  ions were generated with almost the same abundance in the DHB-MALDI mass spectrum of **1** as shown in Figure 3(C). The  $[M + H]^+$  ion were slightly stronger with ASA as compared to that without the matrix, which indicated the reduction of **1**. The CHCA- and FSA-MALDI mass spectra of **1** were almost the same as that without matrix-MALDI. The NSA matrix accelerated the dehydrogenation of **1** because NSA showed hydrogen-accepting ability. In the oxidation/reduction study of peptides in the MALDI process, DAN, ASA, and DHB matrices possess hydrogen-donating properties, while FSA and NSA are hydrogen acceptors, and CHCA may play the role of both acceptor and donor.<sup>22</sup> The tendency was similar, but the  $[M - H]^+$  ions of alkaloids were different from the peptides in MALDI-MS. This was because the oxidation/reduction processes in the MALDI were dependent on the analyte's properties.

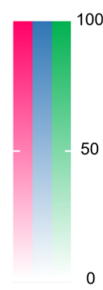
The tendency to shift from  $[M + H]^+$  to  $[M - H]^+$  in **1** was almost the same as in **2** and **3** in the series of MALDI-MS with six matrices (see Supporting Information SI-5 and -6). On the other hand, there were no differences in the series of six-matrix MALDI mass spectra of **4** and **5** (see Supporting Information SI-7 and -8) and the  $[M + H]^+$  ions were predominantly detected, indicating that the molecular ions of **4** and **5** were no reactive to these matrices. The laser-induced alkaloid shifts indicated their oxidation/reduction reactivity. The mass shifts of the molecular ions were sensitive to the specific structure of alkaloids **1**, **2**, and **3** and not to **4** and **5**. Therefore, the dehydrogenation of alkaloids in MALDI-MS was dependent on their structure.

**Indole and Auxin Metabolites.** Indole **6** has a nitrogen atom, which is not linked by a double bond but by C–N–C single bonds in the structural formula. However, dehydrogenation did not proceed in the indole ring. Therefore, we studied the properties of indole compounds **6**–**10** (Figure 1) by MALDI. The molecular ion  $[M]^+$  and protonated molecule  $[M + H]^+$  were observed in the MALDI-MS spectrum of **6** as shown in Table 1 and SI 9–13. A molecular ion is generated in the high aromaticity structure part.<sup>8</sup> The chemical properties of indole are determined by the amine group not possessing Lewis basicity because the lone-pair electron on the nitrogen atom is involved in electron delocalization in the aromatic ring. It was reasonable to assume that dehydrogenation does not proceed in the indole rings. The lone pair electron of nitrogen had to be free and not involved in aromaticity or a delocalized electron system for the laser-induced dehydrogenation of alkaloids.

Indole alkaloids such as auxin or indole-3-acetic acid **7**, indole-3-ethanol **8**, and indole-3-acetamide **9** can be ionized due to their aromaticity as both the molecular ion  $[M]^+$  and the protonated molecule  $[M + H]^+$  are observed in the spectra with the CHCA matrix (Supporting Information SI 9–13).

**Table 1.** Relative Ion Intensities (%) of  $[M - H]^+$ ,  $[M]^{*+}$ , and  $[M + H]^+$  Ions; CHCA-MALDI-MS Data (A) and (B); and FSA-MALDI-MS Data (C)<sup>a</sup>

(A) CHCA matrix				(B) CHCA matrix				(C) FSA matrix			
Compounds	$[M - H]^+$	$[M]^{*+}$	$[M + H]^+$	Compounds	$[M - H]^+$	$[M]^{*+}$	$[M + H]^+$	$[M - H]^+$	$[M]^{*+}$	$[M + H]^+$	
Indole 6	0	100	79	Yohimbine 2	44	15	100	100	33	25	
Indole-3-ethanol 8	5	100	47	Emetine 11	73	27	100	100	35	7	
Indole-3-acetic acid 7	3	100	55	Ajmalicine 12	92	26	100	100	32	8	
Indole-3-acetamide 9	*	45	100	Indapamide 13	57	100	67	28	100	29	
Tryptamine 10	1	1	100	Brucine 14	20	21	100	68	100	20	
				Vincamine 15	24	7	100	21	100	21	
				Antazoline 16	17	10	100	92	31	97	
				Diltiazem 22	3	1	100	34	9	100	
				Cinchonidine 21	1	1	100	24	6	100	
				Epinastine 17	0	0	100	2	1	100	
				Lisinopril 18	0	0	100	0	0	100	
				7-Ethyl-10-hydroxy Camptothecin 19	0	3	100	1	2	100	
				Camptothecin 20	0	1	100	1	5	100	



<sup>a</sup>The ion intensities were normalized to the highest ion as 100% between the three ions. The data are the averages of the relative ion intensities of the five times measurements. The standard deviations are summarized in SI-27. The asterisks mean that the signals of the matrix and alkaloids were overlapped as shown in SI-10 (7) and SI-12 (9).

The alcohol and acetic acid groups were not directly involved in the protonated molecular ionization, and the properties of the indole ring were predominant in the generation of both  $[M + H]^+$  and  $[M]^{*+}$ . On the other hand, only the protonated molecule  $[M + H]^+$  predominated in the MALDI mass spectrum of tryptamine 10 because it contains a base primary amine group as the stable protonated site. Therefore, the mobile proton was required to precede dehydrogenation at the nitrogen atom.

**Reproducibility and Estimation of the Relative Ion Intensity.** We measured the five times MALDI-MS spectra of each alkaloid for each type of data on the same sample spots as shown in SI-14. Only the data of FSA-MALDI-MS of vincamine 15 was obtained three times. Multimatrix variation MALDI-MS of alkaloids were acquired with the five times measurements, SI-15–26. The abundance ratio of the three molecular ions  $[M - H]^+$ ,  $[M]^{*+}$ , and  $[M + H]^+$  was estimated from intensities of the corresponding peaks in MALDI mass spectra of alkaloids. The highest intensity ion was normalized as 100 (%) between the three ions. The average values (%) are shown in SI-27 and Table 1. The standard deviations were less than five (%) except that of 12 in the CHCA-MALDI mass spectra (SI-27). The standard deviations of FSA-MALDI-MS data tended to be higher than those of the CHCA-MALDI-MS data (SI-27). The relative peak intensities  $[M - H]^+$ ,  $[M]^{*+}$ , and  $[M + H]^+$  ions were reproduced high in each data.

**Dehydrogenation Rules of Alkaloids in Their MALDI.** The abundance ratio (%) of the three molecular ions of  $[M - H]^+$ ,  $[M]^{*+}$ , and  $[M + H]^+$  is summarized in Table 1 (Supporting Information SI-15–27). From the abundance of the dehydrogenated ion  $[M - H]^+$ , the reactivity of alkaloids was categorized into three categories roughly—the highly reactive ones such as 1–3 and 11–16 (Table 1), the middle reactive ones such as 21 and 22, and the low reactive ones such

as 4, 5, and 17–20 and 6–10 (Table 1). The dehydrogenated ions  $[M - H]^+$  were generated by MALDI from the cyclic and single bonded amines of alkaloids such as emetine 11, ajmalicine 12, indapamide 13, brucine 14, vincamine 15, and antazoline 16. None of them contains the primary amine as the stable protonated site. The sulfonamide group in 13 does not possess the basicity due to the sulfo groups and it was not the stable protonated site. The proton dehydrogenation process is linked to the reactive nitrogen atoms.

On the other hand, epinastine 17 and lisinopril 18 contain the stable protonated site in their structure such as the basic primary amine. They were not dehydrogenated even though they contain the other reactive nitrogen atoms. Camptothecin 19 and 7-ethyl-10-hydroxycamptothecin 20 have a quinoline possessing the same basicity as the protonated site, suppressing the dehydrogenation. Additionally, the electron-withdrawing groups neighboring the nitrogen hindered the dehydrogenation because the lone pair of the nitrogen atom did not induce the reaction directly. Cinchonidine 21 also involves a quinoline, but the tertiary amine is without the neighboring electron-withdrawing groups. Diltiazem 22 contains the noncyclic or cyclic tertiary amines, and the cyclic one neighbors the aromatic ring and ketone group. Their dehydrogenation proceeded weakly as shown in Table 1. The partial dehydrogenation was observed with 21 and 22. We compared the alkaloid mass shifts in the MALDI-MS spectra with CHCA and FSA matrices (Table 1). The dehydrogenation with FSA proceeded better than that with CHCA in MALDI of 1 (Figure 3). Compounds 21 and 22 were clearly classified as middle reactive alkaloids following the alkaloid mass shift tables with the CHCA and FSA matrices. The dehydrogenation was the reaction of the alkaloid analytes and matrices. The matrices controlled the reactivity of alkaloids under laser irradiation, which was a new function of matrix in

MALDI-MS. Here, it is important for us to investigate new functional matrices such as a reaction inducer to develop more fine structure analysis.

**Discrimination of Structural Isomers of Alkaloids.** Alkaloids **2** and **15** had the same molecular formula ( $C_{21}H_{26}N_2O_3$ ) (Supporting Information SI-2) and were structural isomers. We tried to discriminate between **2** and **15** using the alkaloid reactivity of dehydrogenation in various matrix MALDI-MS (see Supporting Information SI-5 and -19). The reactivity of **2** was 44% of the  $[M - H]^+$  intensity, and it was higher than that of **15** (24%) in CHCA-MALDI mass spectra (Table 1). In addition, the isomeric alkaloids **2** and **15** were clearly discriminated in the FSA-MALDI mass spectra; the  $[M]^{*+}$  ion of **15** was predominant and the  $[M - H]^+$  ion of **2** was predominant (Table 1 and Supporting Information SI-5 and -19). The nitrogen atom of the indole ring in **2** was a secondary amine and that of **15** was a tertiary amine. Compound **15** had higher aromaticity at the indole ring than **2**. Thus, the molecular ion  $[M]^{*+}$  of **15** was generated predominantly. The alkaloid reactivity analysis using matrix-variation MALDI-MS was useful for the discrimination of the structural isomers of alkaloids.

## CONCLUSION

The dehydrogenation of alkaloids proceeded by MALDI as their in-source decay reaction. The alkaloids were classified into those with high, middle, and low reactivity according to their molecular related ions. The ion abundance ratio of  $[M - H]^+$ ,  $[M]^{*+}$ , and  $[M + H]^+$  was taken as the indicator of alkaloid reactivity with the multimatrix variation MALDI-MS. The dehydrogenation of alkaloids was used for the prediction of their structure around the nitrogen bondings. The alkaloid isomers were also discriminated based on the reactivity difference between alkaloid and matrices.

## ASSOCIATED CONTENT

### Supporting Information

The Supporting Information is available free of charge at <https://pubs.acs.org/doi/10.1021/jasms.2c00221>.

Molecular formula and monoisotopic molecular masses (SI-1); laser powers (SI-2); matrix structure (SI-3); entire mass spectra of **1** (SI-4); mass spectra of yohimbine **2** (SI-5); mass spectra of tryptoline **3** (SI-6); mass spectra of harmaline **4** (SI-7); mass spectra of harmine **5** (SI-8); mass spectrum of indole **6** (SI-9); mass spectrum of indole-3-acetic acid **7** (SI-10); mass spectrum of indole-3-ethanol **8** (SI-11); mass spectrum of indole-3-acetamide **9** (SI-12); mass spectrum of tryptamine **10** (SI-13); mass spectra of five repeated measurements of **1** (SI-14); mass spectra of emetine **11** (SI-15); mass spectra of ajmalicine **12** (SI-16); mass spectra of indapamide **13** (SI-17); mass spectra of bruchine **14** (SI-18); mass spectra of vincamine **15** (SI-19); mass spectra of antazoline **16** (SI-20); mass spectra of epinastine **17** (SI-21); mass spectra of lisinopril **18** (SI-22); mass spectra of camptothecin **19** (SI-23); mass spectra of 7-ethyl-10-hydroxycamptothecin **20** (SI-24); mass spectra of cinchonidine **21** (SI-25); mass spectra of diltiazem **22** (SI-26); table of the averages of the relative ion intensities (%) and the standard deviations (SI-27) (PDF)

## AUTHOR INFORMATION

### Corresponding Author

Tohru Yamagaki – Bioorganic Research Institute, Suntory Foundation for Life Sciences, Soraku-gun, Kyoto 619-0284, Japan; [orcid.org/0000-0001-7463-3255](https://orcid.org/0000-0001-7463-3255); Email: [yamagaki@sunbor.or.jp](mailto:yamagaki@sunbor.or.jp)

### Authors

Tsukihiko Osawa – Bioorganic Research Institute, Suntory Foundation for Life Sciences, Soraku-gun, Kyoto 619-0284, Japan

Kohki Fujikawa – Bioorganic Research Institute, Suntory Foundation for Life Sciences, Soraku-gun, Kyoto 619-0284, Japan; [orcid.org/0000-0002-7929-3314](https://orcid.org/0000-0002-7929-3314)

Takehiro Watanabe – Bioorganic Research Institute, Suntory Foundation for Life Sciences, Soraku-gun, Kyoto 619-0284, Japan

Kohtaro Sugahara – Bioorganic Research Institute, Suntory Foundation for Life Sciences, Soraku-gun, Kyoto 619-0284, Japan; [orcid.org/0000-0003-3812-1521](https://orcid.org/0000-0003-3812-1521)

Complete contact information is available at: <https://pubs.acs.org/10.1021/jasms.2c00221>

### Notes

The authors declare no competing financial interest.

## REFERENCES

- Groseclose, M. R.; Andersson, M.; Hardesty, W. M.; Caprioli, R. M. Identification of proteins directly from tissue: in situ tryptic digestions coupled with imaging mass spectrometry. *J. Mass Spectrom.* **2007**, *42*, 254–262.
- Shimma, S.; Sugiura, Y.; Hayasaka, T.; Hoshikawa, Y.; Noda, T.; Setou, M. MALDI-based imaging mass spectrometry revealed abnormal distribution of phospholipids in colon cancer liver metastasis. *J. Chromatogr. B Analyt. Technol. Biomed. Life Sci.* **2007**, *855*, 98–103.
- Cornett, D. S.; Frappier, S. L.; Caprioli, R. M. MALDI-FTICR imaging mass spectrometry of drugs and metabolites in tissue. *Anal. Chem.* **2008**, *80*, 5648–5653.
- Boughton, B. A.; Thinakaran, D.; Sarabia, D.; Bacic, A.; Roessner, U. Mass spectrometry imaging for plant biology: a review. *Phytochem. Rev.* **2016**, *15*, 445–488.
- Yamamoto, K.; Takahashi, K.; Mizuno, H.; Anegawa, A.; Ishizaki, K.; Fukai, H.; Ohnishi, M.; Yamazaki, M.; Masujima, T.; Mimura, T. Cell-specific localization of alkaloids in *Catharanthus roseus* stem tissue measured with imaging MS and single-cell MS. *Proc. Natl. Acad. Sci. U.S.A.* **2016**, *113*, 3891–3896.
- Nakabayashi, R.; Hashimoto, K.; Toyooka, K.; Sato, K. Top-down metabolomic approaches for nitrogen-containing metabolites. *Anal. Chem.* **2017**, *89*, 2698–2703.
- Sugahara, K.; Kitao, K.; Watanabe, T.; Yamagaki, T. Imaging mass spectrometry analysis of flavonoids in blue viola petals and their enclosure effects on violanin during color expression. *Anal. Chem.* **2019**, *91*, 896–902.
- Yamagaki, T.; Watanabe, T. Hydrogen radical removal causes complex overlapping isotope patterns of aromatic carboxylic acids in negative-ion matrix-assisted laser desorption/ionization mass spectrometry. *Mass Spectrom. (Tokyo)* **2012**, *1*, A0005.
- Barber, M.; Bell, D.; Eckersley, M.; Morris, M.; Tetler, L.; Derrick, P. J. The use of m-nitrobenzyl alcohol as a matrix in Fast Atom Bombardment mass spectrometry. *Rapid Commun. Mass Spectrom.* **1988**, *2*, 18–21.
- Takayama, M.; Fukai, T.; Nomura, T. Effect of a new matrix system for low-polar organic compounds in Fast Atom Bombardment mass spectrometry. *J. Mass Spectrom. Soc. Jpn.* **1988**, *36*, 169–173.

(11) Takayama, M.; Kosaka, T.; Kinoshita, T. Formation of  $[M-H]^+$  ions under Fast Atom Bombardment conditions: Trolox and a-tocopherol. *J. Mass Spectrom. Soc. Jpn.* **1996**, *44*, 473–481.

(12) Grigsby, R. D.; Scheppelle, S. E.; Grindstaff, Q. G.; Sturm, G. P. Jr.; Taylor, L. C. E.; Tudge, H.; Wakefield, C.; Evans, S. Evaluation of Fast Atom Bombardment mass spectrometry for identification of nitrogen-containing compounds in fossil fuels. *Anal. Chem.* **1982**, *54*, 1108–1113.

(13) Yamagaki, T.; Takeuchi, M.; Watanabe, T.; Sugahara, K.; Takeuchi, T. Mechanism for odd-electron anion generation of dihydroxybenzoic acid isomers in matrix-assisted laser desorption/ionization mass spectrometry with density functional theory calculations. *Rapid Commun. Mass Spectrom.* **2016**, *30*, 2650–2654.

(14) Yamagaki, T.; Watanabe, T.; Tanaka, M.; Sugahara, K. Laser-induced hydrogen radical removal in UV MALDI-MS allows for the differentiation of flavonoid monoglycoside isomers. *J. Am. Soc. Mass Spectrom.* **2014**, *25*, 88–94.

(15) Sekiya, S.; Yamaguchi, Y.; Kato, K.; Tanaka, K. Mechanistic elucidation of the formation of reduced 2-aminopyridine-derivatized oligosaccharides and their application in matrix-assisted laser desorption/ionization mass spectrometry. *Rapid Commun. Mass Spectrom.* **2005**, *19*, 3607–3611.

(16) Nonami, H.; Tanaka, K.; Fukuyama, Y.; Erra-Balsells, R.  $\beta$ -Carboline alkaloids as matrices for UV-Matrix-assisted laser desorption/ionization Time-of-flight mass spectrometry in positive and negative ion modes. Analysis of proteins of high molecular mass, and of cyclic and acyclic oligosaccharides. *Rapid Commun. Mass Spectrom.* **1998**, *12*, 285–296.

(17) Nonami, H.; Wu, F.; Thummel, R. P.; Fukuyama, Y.; Yamaoka, H.; Erra-Balsells, R. Evaluation of pyridoindoles, pyridylindoles and pyridylpyridoindoles as matrices for ultraviolet matrix-assisted laser desorption/ionization time-of-flight mass spectrometry. *Rapid Commun. Mass Spectrom.* **2001**, *15*, 2354–2373.

(18) Strupat, K.; Karas, M.; Hillenkamp, F. 2,5-Dihydroxybenzoic acid: a new matrix for laser desorption/ionization mass spectrometry. *Int. J. Mass Spectrom. Ion Processes* **1991**, *111*, 89–102.

(19) Beavis, R. C.; Chaudhary, T.; Chait, B. T.  $\alpha$ -Cyano-4-hydroxycinnamic acid as a matrix for matrix-assisted laser desorption mass spectrometry. *Org. Mass Spectrom.* **1992**, *27*, 156–158.

(20) Juhasz, P.; Costello, C. E. Matrix-assisted laser desorption ionization time-of-flight mass spectrometry of underivatized and permethylated gangliosides. *J. Am. Soc. Mass Spectrom.* **1992**, *8*, 785–796.

(21) Sakakura, M.; Takayama, M. In-source decay and fragmentation characteristics of peptides using 5-aminosalicylic acid as matrix in matrix-assisted laser desorption/ionization mass spectrometry. *J. Am. Soc. Mass Spectrom.* **2010**, *21*, 979–988.

(22) Asakawa, D.; Takayama, M.  $C\alpha$ -C Bond cleavage of the peptide backbone in MALDI in-source decay using salicylic acid derivative matrices. *J. Am. Soc. Mass Spectrom.* **2011**, *22*, 1224–1233.

(23) Fukuyama, Y.; Iwamoto, S.; Tanaka, K. Rapid sequencing and disulfide mapping of peptides containing disulfide bonds by using 1,5-diaminonaphthalene as reductive matrix. *J. Mass Spectrom.* **2006**, *41*, 191–201.